# Supporting Information

## Ohno et al. 10.1073/pnas.0906551107

### SI Materials and Methods

**Organotypic Slice Culture.** Cocultures of sensorimotor Cx and cervical cord slices were prepared essentially as previously described (1, 2). Briefly, 350-μm-thick coronal cortical and axial SpC slices were sectioned from P0 C57BL/6 mice using a Microslicer (Dosaka EM), and the forelimb areas were dissected from the cortical sections in chilled cutting solution (120 mM choline, 3 mM KCl, 1.25 mM $NaH_2PO_4$, 28 mM $NaHCO_3$, 8 mM $MgCl_2$, and 25 mM glucose). The slices were placed on a collagen-coated membrane (Transwell-Col, 3.0-μm pore; Costar) and maintained at 37 °C under humidified 95% air and 5% $CO_2$. For pharmacological experiments (Fig. S1), 50 μM APV and 10 μM ifenprodil were added to the culture medium from 6 to 12 DIV (3); the drug-containing medium was then replaced with drug-free medium, and electrophysiological studies were carried after an additional 24 h. The medium was changed twice a week, and fresh drugs were added with each replacement. In heterotypic cocultures, the slices from WT mice and one of the two types of KO mice ($2b^{-/-}$ or $2a^{-/-}$) were cocultured.

**Electrophysiological Study.** For the electrophysiological study (2), slices from the culture insert with its membrane were placed in a recording chamber and superfused with artificial cerebrospinal fluid (ACSF) containing 119 mM NaCl, 2.5 mM KCl, 1 mM $NaH_2PO4$, 26 mM $NaHCO_3$, 1.29 mM $MgSO_4$, and 2.24 mM $CaCl_2$ saturated with 95% $O_2$ and 5% $CO_2$. Current pulses (500-μA amplitude, 100-μs width) were then applied at a frequency of 0.1 Hz to the deeper layers of the cortical slices using a bipolar electrode. CS field EPSPs were recorded at 80-μm intervals along a lattice within the spinal gray matter using a glass micropipette filled with 2M NaCl (2–3 MΩ) (Fig. S1*A*, *Inset*). The slices cultured in drug-containing medium were washed with the superfusate for more than 15 min in the recording chamber.

CS EPSCs were evoked utilizing the same local stimulation electrode used for field EPSPs. The internal solution in the patch pipettes contained 128 mM Cs-gluconate, 20 mM CsCl, 10 mM Hepes-CsOH (pH 7.2–3), 0.2 mM EGTA, 2 mM ATP ($Mg^{2+}$ salt), and 0.2 mM GTP ($Na^+$ salt). Osmolarity was adjusted to 280 mOsm. AMPA and NMDA currents were recorded in the presence of 50 μM picrotoxin in ACSF at holding potentials of −70 mV and +40 mV, respectively. This separation of the two components of the EPSC was confirmed in some experiments by applying either APV or CNQX to isolate the AMPA and NMDA conductances, respectively. Cells in which the series resistance was >30 MΩ or the leak current was >100 pA were excluded from our analysis. Decay times (0.37 peak amplitude) and the averaged amplitudes of the EPSCs were measured using Clampfit (Axon Instruments).

**Anterograde Labeling of CS Axons.** For anterograde labeling of CS axons (2), Biocytin (Sigma) was placed on deep cortical layers 24 h before fixation with 4% paraformaldehyde and 0.5% glutaraldehyde. The slices were then reacted overnight at 4 °C in an avidin/biotinylated enzyme solution (ABC kit; Vector Laboratories) in 100 mM PBS also containing 0.1% Triton and 0.1% BSA. Labeled cells were visualized using nickel-intensified diaminobenzidine (Dojindo) and β-D-glucose/glucose oxidase. To measure regional axonal arborization, two lines were drawn so that they divided the SpC along the dorsoventral axis 2:8 (traversing the dorsal area) and 7:3 (traversing the ventral area) (Fig. S4*B*). The numbers of cortical fibers crossing the lines that traversed the dorsal or ventral SpC were counted by changing the plane of focus. Fiber density was then calculated by dividing the number of fibers counted by the length of the line.

**Optical Recordings.** For optical recordings (4), the slices were stained with the voltage-sensitive dye Di-4-ANNEPS (0.2 mM; Molecular Probes), after which changes in the fluorescence evoked by cortical stimulation at 0.1 Hz were recorded using a high-speed CCD camera system (MiCAM02; Brainvision, Inc.), and at least 49 responses were averaged (Fig. S2*A*). Slices were incubated with the dye for 25–30 min in an oxygen-saturated moist chamber and then placed in a perfusion chamber mounted on the stage of a fluorescence microscope (BX50WI; Olympus). After bubbling the stained slices with 100% $O_2$ for 60 min, they were rinsed with ACSF (135 mM NaCl, 2.5 mM KCl, 2 mM $CaCl_2$, 1.25 mM $MgCl_2$, 10 mM Hepes, 25 mM glucose, pH 7.35). The intensity of the Di-4-ANNEPS fluorescence at each pixel was divided by the intensity of the brightest pixel in the image to obtain the normalized fluorescence, after which the percent fractional change in normalized fluorescence (%ΔF/F) was calculated and used as the optical signal. For quantitative measurements, two ROIs were selected from dorsal and ventral areas of each hemi-SpC (Fig. 3*A*, *Inset*).

**Quantitative Evaluation of Fluorescence Intensity.** For quantitative evaluation, ImageJ (National Institutes of Health) was used to measure the mean fluorescence intensity of the dorsal and ventral areas, which were selected based on the same criteria described for the optical imaging (Fig. 2*A*). We estimated relative fiber density in the ventral area as the ventrodorsal ratio of the mean fluorescence intensities. To obtain clearer images for the figures (Fig. 3), we adjusted the brightness and contrast using Photoshop Version 6.0 (Adobe) after quantitative measurements were complete. For quantitative comparison of mean fluorescence intensity and optical signal intensity, the SpC was divided into 16 ROIs in a 4 × 4 lattice-like pattern and the intensities of the optical EPSPs and the relative fiber densities in each ROI were compared (4). Spearman's rank correlation coefficients were used for the statistical analysis.

All animal experiments were performed in accordance with Ethical Committee Guidelines for Animal Experimentation, Teikyo University School of Medicine (No. 07-045), and the National Institutes of Health Guide for the Care and Use of Laboratory Animals (National Institutes of Health Publication No. 80-23) revised in 1996. All efforts were made to minimize the number of animals used and their suffering.


1. Takuma H, Sakurai M, Kanazawa I (2002) *In vitro* formation of corticospinal synapses in an organotypic slice co-culture. *Neuroscience* 109:359–370.
2. Ohno T, Maeda H, Sakurai M (2004) Regionally specific distribution of corticospinal synapses because of activity-dependent synapse elimination in vitro. *J Neurosci* 24: 1377–1384.
3. Ohno T, Sakurai M (2005) Critical period for activity-dependent elimination of corticospinal synapses in vitro. *Neuroscience* 132:917–922.
4. Maeda H, Ohno T, Sakurai M (2007) Optical and electrophysiological recordings of corticospinal synaptic activity and its developmental change in in vitro rat slice cocultures. *Neuroscience* 150:829–840.

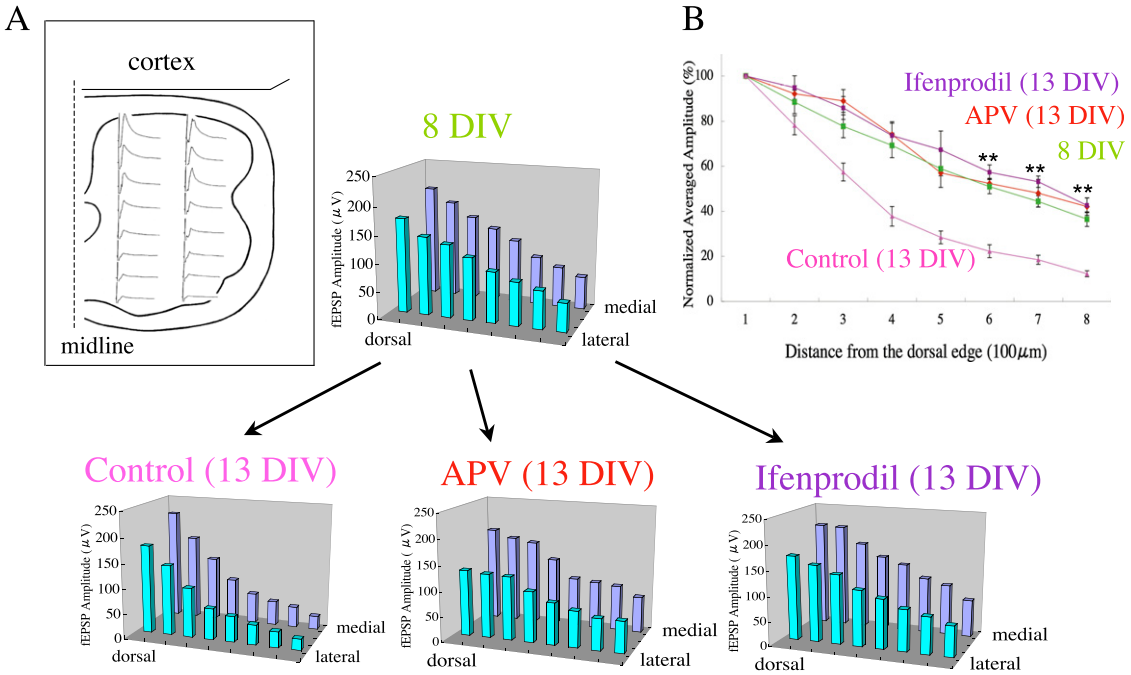


**Fig. S1.** GluN2B-dependent synapse elimination in the ventral area. (*A*) Spatial distribution of field EPSPs recorded at 80-μm intervals along a lattice in the spinal gray matter at 13 DIV. (*Inset*) Averaged field EPSP amplitudes at each point of the lattice ($n$ = 12). Synapse elimination on the ventral side seen in control cultures at 13 DIV was similarly blocked by ifenprodil and APV. (*B*) Dorsoventral gradient between the normalized and averaged field EPSP amplitudes recorded at two mediolateral points at 8 DIV and 13 DIV, with or without APV or ifenprodil. There are significant differences in the ventral five points between the untreated control cultures and those treated with APV or ifenprodil (**$P$ < 0.01, ANOVA followed by the Dunnett test for multiple comparison).

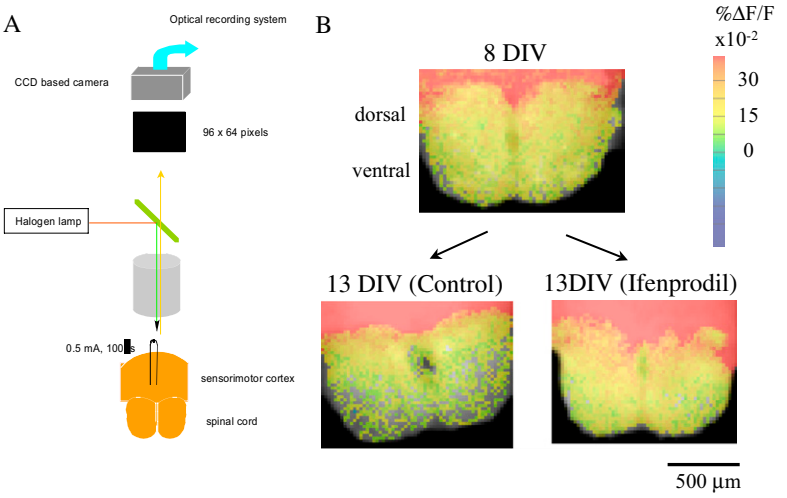


**Fig. S2.** Optical recordings of CS EPSPs. (*A*) Schematic illustration of the optics and camera system used for recording optical EPSPs. Light from a halogen lamp passes through an excitation filter and is reflected from a dichroic mirror onto the culture preparation. Longer wavelength fluorescent emission is collected by the objective, captured through an absorption filter, and projected onto a CCD device with an 8.4 × 6.5-mm$^2$ imaging area made up of 96 × 64 pixels. The software supplies the trigger signal leading to electrical stimulation of a deep layer of the cortical slice. (*B*) Spatial patterns of synaptic responses at their peak viewed from above. Developmental changes in the responses with and without ifenprodil are shown. Reduction of the ventral intensity at 13 DIV is seen in the control culture but is blocked by ifenprodil. The pseudocolor bar indicates signal intensity [percent fractional change in normalized fluorescence (%ΔF/F)]. (Scale bar: 500 μm.)

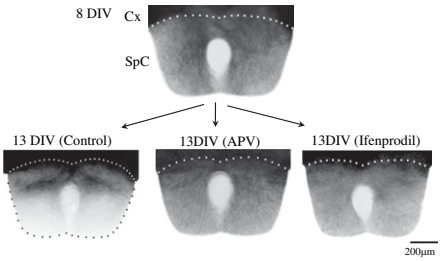


**Fig. S3.** GluN2B-dependent axonal regression from the ventral area. Anterograde labeling of cortical efferent axons with biocytin at 8 DIV and 13 DIV, with or without APV or ifenprodil. Small amounts of biocytin powder were placed on cortical slices at 7 or 12 DIV. Axonal regression on the ventral side seen at 13 DIV in the control culture was blocked by APV or ifenprodil. (Scale bar: 200 μm.) To obtain clearer images, we adjusted the brightness level using Photoshop Version 6.0 to reduce the background.

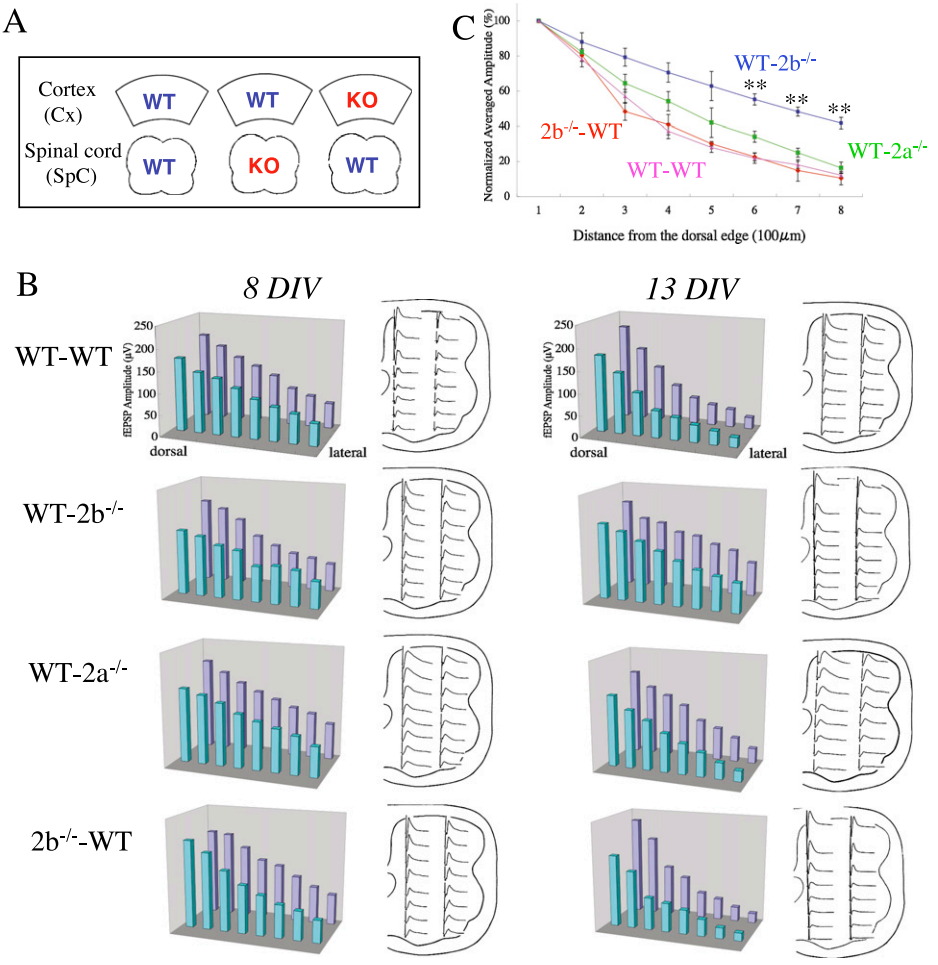


**Fig. S4.** Spatial distribution of CS field EPSPs in heterotypic cocultures. (*A*) We used three types of heterotypic cocultures: (*i*) WT Cx and SpC (*Left*), (*ii*) WT Cx with KO ($2b^{-/-}$ or $2b^{-/-}$) SpC (*Center*), and (*iii*) $2b^{-/-}$ Cx with WT SpC (*Right*). (*B*) Spatial distribution of averaged field EPSPs traces (*Right*) and their amplitudes (*Left*) at 8 and 13 DIV in the indicated heterotypic. In WT-$2b^{-/-}$ pairs, mean amplitudes of EPSPs recorded at two points in the ventral area (the second and third rows from the ventral-most row) at 8 and 13 DIV were 81.9 ± 1.7 μV and 98.3 ± 10.3 μV, respectively (mean ± SD, $n = 12$; $P > 0.5$). In WT-$2a^{-/-}$ pairs, mean EPSP amplitudes in the ventral area at 8 and 13 DIV were 97.8 ± 4.8 μV and 36.3 ± 2.8 μV, respectively ($n = 12$; $P < 0.01$). In $2b^{-/-}$-WT pairs, mean EPSP amplitudes in the ventral area at 8 and 13 DIV were 80.8 ± 6.1 μV and 36.3 ± 2.8 μV, respectively ($n = 12$; $P < 0.01$) (*C*) Dorsoventral gradient between the normalized and averaged amplitudes of field EPSPs recorded at two mediolateral points at 13 DIV in each pair. Note the significant differences in the ventral points between the WT-$2b^{-/-}$ and control pairs ($n = 12$; $P < 0.01$, ANOVA followed by the Dunnett test for multiple comparison). Similarly, there was a significant difference in the ventral areas between WT-$2b^{-/-}$ and WT-$2a^{-/-}$ pairs ($n = 12$; $P < 0.01$, ANOVA followed by Scheffé's method for multiple comparison). There was, however, no significant difference between the $2b^{-/-}$-WT and control pairs ($n = 12$; $P > 0.5$, ANOVA). $^{**}P < 0.01$.

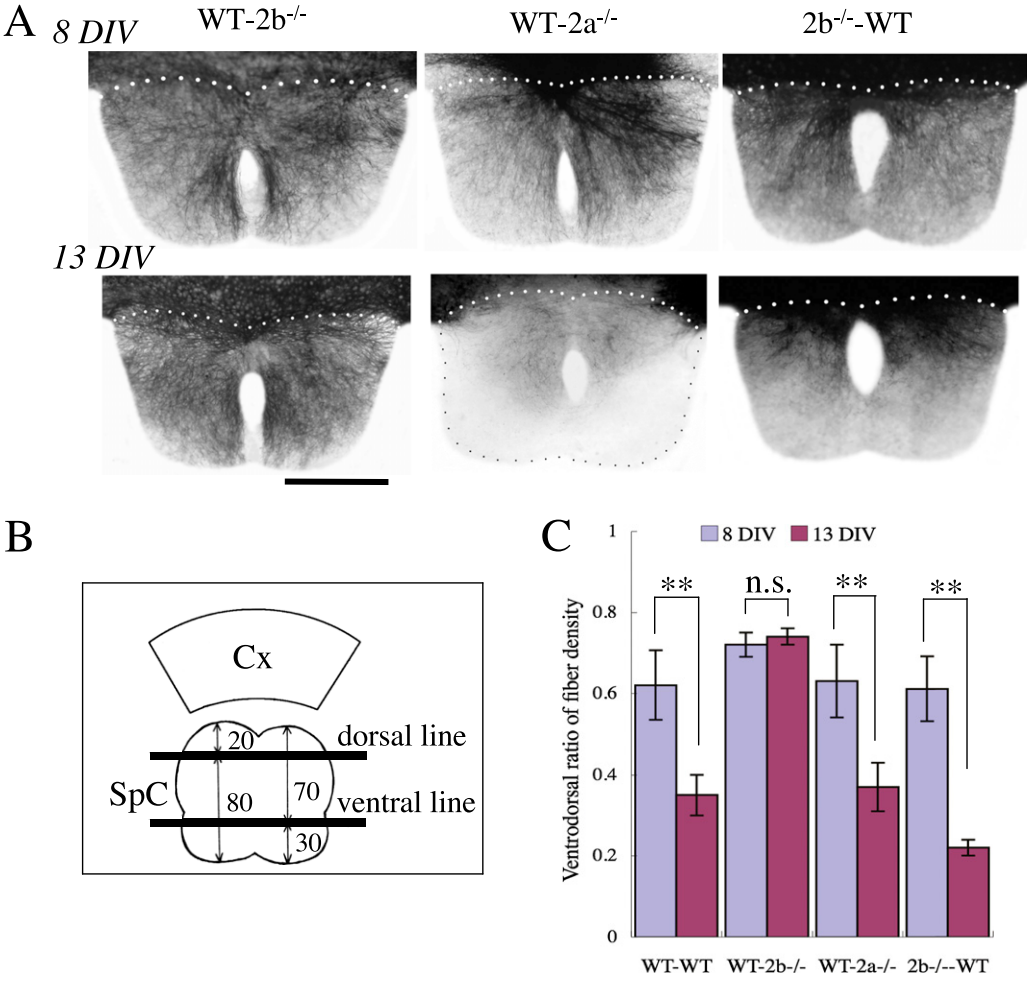


**Fig. S5.** Quantitative analysis of cortical efferent axons anterogradely labeled with biocytin. (*A*) At 8 DIV, axon terminals were distributed throughout the spinal gray matter in all cocultures. At 13 DIV, axon terminals in the WT-$2a^{-/-}$ and $2b^{-/-}$-WT cultures were restricted to the dorsal area but the elimination of axon terminals in the ventral area was blocked in WT-$2b^{-/-}$ cultures. In WT-$2b^{-/-}$ pairs, the number of cortical fibers per millimeter of dorsal vs. ventral area (d vs. v) was 339.0 ± 38.6 vs. 244.3 ± 25.1 (mean ± SEM, $n = 6$; $P > 0.5$) at 8 DIV and 365.6 ± 28.5 vs. 270.5 ± 21.3 ($n = 6$; $P > 0.5$) at 13 DIV. In WT-$2a^{-/-}$ pairs, d vs. v at 8 DIV was 302.6 ± 25.6 vs. 190.6 ± 20.3 ($n = 6$; $P > 0.5$), and at 13 DIV, it was 359.3 ± 21.2 vs. 132.9 ± 13.2 ($n = 6$; $P < 0.01$). In $2b^{-/-}$-WT pairs, d vs. v at 8 DIV was 313.7 ± 28.5 vs. 194.0 ± 23.7 ($n = 6$; $P > 0.5$), and at 13 DIV, it was 416.0 ± 17.9 vs. 91.5 ± 7.1 ($n = 6$; $P < 0.01$). (Scale bar: 500 μm.) (*B*) Schematic drawing showing the fiber-counting method. The 20% line was used to count axons in the dorsal area, and the 70% line was used to count those in the ventral area. (*C*) Ventrodorsal ratios of the numbers of cortical fibers per millimeter. The ratio at 13 DIV was smaller than that at 8 DIV in WT-WT, WT-$2a^{-/-}$, and $2b^{-/-}$-WT cocultures ($n = 6$; $^{**}P < 0.01$), but there was no significant change in WT-$2b^{-/-}$ cocultures ($n = 6$; $P > 0.5$). n.s., Not significant.

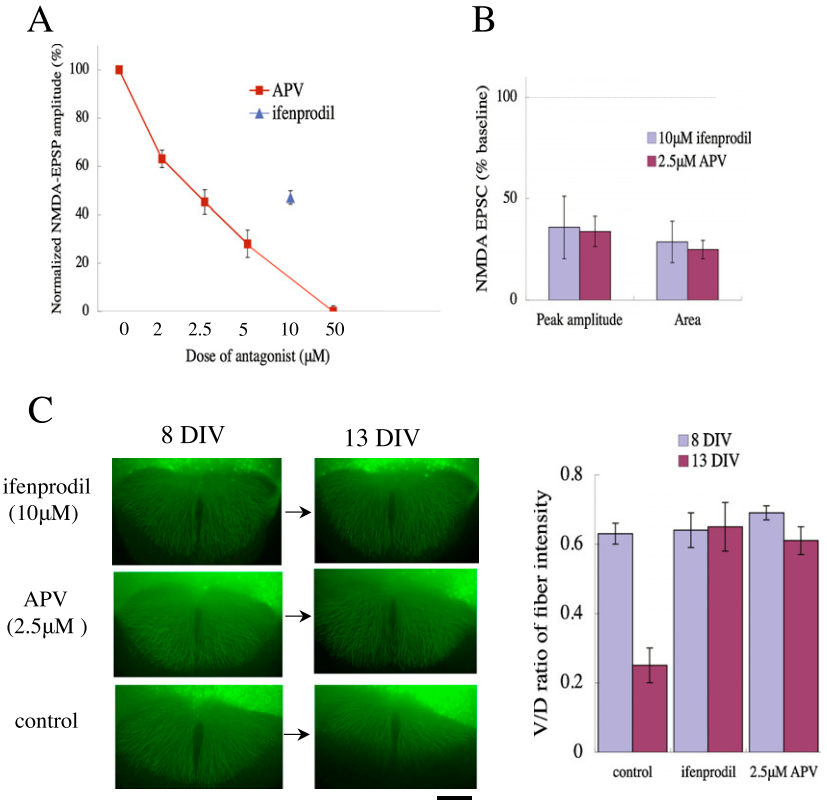


**Fig. S6.** Effect of manipulation of NMDA EPSC on the synapse elimination in WT SpC. (*A*) Reduction of the peak amplitudes of NMDAR field EPSPs in the presence of APV (red squares) and ifenprodil (blue triangle). (*B*) No significant difference was found between reductions in NMDAR EPSCs (percentage of the control value) elicited by 2.5 μM APV and 10 μM ifenprodil. Assessed were peak EPSC amplitudes and total areas. (*C*) Live imaging showing the blocking effect of 2.5 μM APV on the elimination process. (Scale bar: 500 μm.)

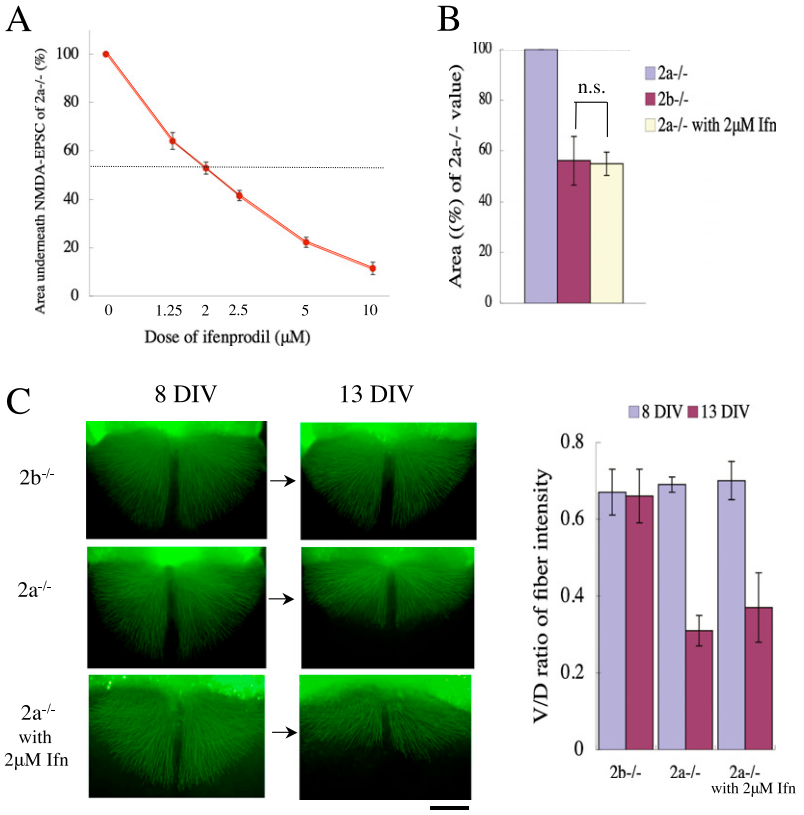


**Fig. S7.** Effect of manipulating NMDA EPSCs on synapse elimination in $2a^{-/-}$ SpC. (*A*) Reduction in the area underneath NMDA EPSC in $2a^{-/-}$ with ifenprodil. The dotted line indicates the % area of the NMDA EPSC in $2b^{-/-}$. (*B*) Application of 2 μM ifenprodil reduced the area of the NMDA EPSC in $2a^{-/-}$ to the same level as that in $2b^{-/-}$. (*C*) Live imaging showing that treating $2a^{-/-}$ with 2 μM ifenprodil did not block ventral synapse elimination. (Scale bar: 500 μm.)